Available online at www.sciencedirect.com

ScienceDirect

Procedia Manufacturing 24 (2018) 74–79

Procedia MANUFACTURING

www.elsevier.com/locate/procedia

4th International Conference on System-Integrated Intelligence

Concept And Design Of A Spherical Joint Mechanism For Service Robots

Tim Froehlich[a,*], Dr. Ulrich Reiser[a], Felix Meßmer[a], Prof. Dr.-Ing. Alexander Verl[b]

[a] *Mojin Robotics GmbH, Panoramaweg 5/1, 71111 Waldenbuch, Germany*

[b] *University Stuttgart, Institute for Control Engineering of Machine Tools and Manufacturing Units, Seidenstr. 36, 70174 Stuttgart, Germany*

Abstract

Robots in daily human environments need to fulfill a lot of requirements and boundary conditions to be accepted and useful. To meet these, in this paper, a mechanism similar to a spherical joint is proposed and compared to others. It can be used to extend the workspace of manipulators and add a wide coverage for sensors mounted on the head of the system while being safe by design and enabling an agile and expressive display of gestures. Beside a generic description of the geometry and the main dimensions of the mechanism, also the kinematic calculation and properties of the workspace are shown and discussed.

Keywords: Service robots; Kinematics; Spherical joint; Robotics

1. Introduction

Since some years the number of applications of robots is constantly increasing. The absolute number of service robots is small compared to industrial applications but has a strong growth rate [1]. To address a wider range of economic profitable applications, on the one hand capabilities need to be extended e.g. gasping on the floor and in normal shelves. On the other hand real world conditions needs to be concidered like safety also for children and disabeled people or the fear of machines. To achieve that a new joint mechanism presented in [2] is analyzed, compared to others and properties are discussed. It can be used between the mobile base of a robot and a manipulator unit as torso joint or as head joint. The mechanism allows a design that is on the one hand safe and on the other hand able to perform agile gestures to reduce fear and gain curiosity. To enable many applications and designs, the basic mechanism is described and compared to others in matters of relevant general measures like the space used for the design. Further, the calculation of the kinematics is described and generalised properties of the achieved workspace are discussed.

* Corresponding author. Tel.: +49-0711-21950973
E-mail address: tim.froehlich@mojin-robotics.de

2351-9789
10.1016/j.promfg.2018.06.011

1.1. Related Work

On a closer look, there are predominantly two types of joints used as torso and head joint in service robots. This is on the one hand a vertical mounted linear joint and on the other hand a combination of revolute joint in a pan-tilt configuration.
Examples for robots using linear joints are the RB1 by Robotnik [3], the PR2 by Willow Garage [4] and the AMIGO by the Eindhoven University of Technology [5]. Here the joint has only limited influence on the extension of the workspace of the arms since the arm needs to overcome the footprint of the platform to grasp an object on the floor. One major disadvantage is that the available space inside the robot is limited to the lowest position of the vertical axis. Due to the fact that parts of the robot move towards each other, this joint type is prone to the danger of crushing hazards. One advantage is that the static stability is maintained in all positions. Linear axes do not suit as head joints.
Other robots use a single Degree of Freedom (DoF) as torso joint like the industrial work assistant Nextage by Kawada [6] or Boston Dynamics' ATLAS [9] as tilt joint for the cameras.
Combinations of revolute joints can be found in pan-tilt configurations as torso joint e. g. in ASIMO by Honda [7] or in REEM and REEM-C by PAL Robotics [8]. Also head-joints are mostly pan-tilt configurations like in the RB1 [3], PR2 [4], AMIGO [5], Nextage [6], ASIMO [7], Hollie [10], REEM and REEM-C [8]. One drawback is that sensors either need to be mounted on a tilting lever or the tilting axis needs to be shifted to the front of the robot to be able to see the floor in front of the robot. The first type increases the height of the robot and the second leads to the danger of clamping hazards.
Some head joints developed to display gestures use an additional roll axis like EMYS (**EM**otive head**Y** **S**ystem) head of the robot FLASH [12] and ERICA by Telecommunications Research Institute International (ATR) [13]. Another design used as torso joint in Hollie by FZI [10] and Justin by DLR [11] and as head joint in Care-O-bot 3 by Fraunhofer IPA [14] consist of a pan-tilt-tilt configuration while the tilt joints are connected by rods. This allows an additionally vertical movement like a scissors lift. This design needs all the space between the mobile base and the manipulator unit and is prone to the danger of crushing hazards or needs a difficult coverage or a costly sensor surveillance of the moving parts.
It can be asserted that different designs with different properties exist but non of them fulfills the goals of a wide sensor coverage also to the floor, agile performance of gestures, a design that supports safety certification and compact construction space.

2. Geometry of the Spherical Joint

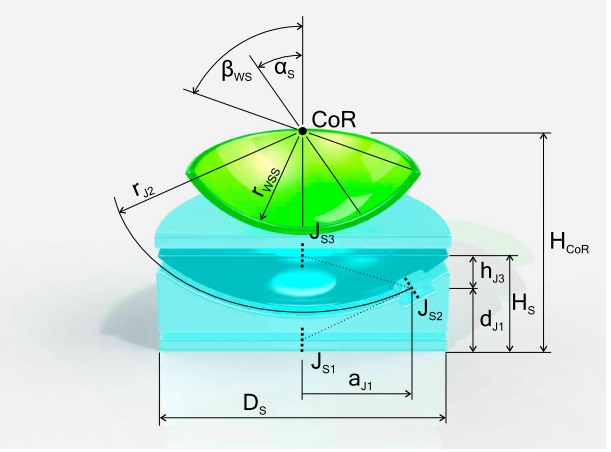

Fig. 1. Geometry and main measures of the spherical joint

The proposed mechanism constitutes a spherical joint by linked mechanism consisting of three independent axes (J_{Si} in figure 1). The first axis J_{S1} is a vertical, panning axis. The second axis J_{S2} is angular aligned by an angle α_S and shifted in horizontal direction by the distance a_{J1}. To achieve the spherical character, the slit of the second axis J_{S2} takes the shape of a section of a sphere marked with the radius r_{J2}. Due to that shape the second axis J_{S2} needs to be shifted vertically by d_{J1}. The third axis J_{S3} is shifted horizontally by the same distance a_{J1} and is congruent with J_{S1} in the upright position of the joint (s. figure 1). Depending on the concrete design, the vertical shift of the third axis h_{J3} can be positive or negative. The geometric relation of axis J_{S1} and J_{S2} defines the center of rotation (CoR). The CoR is located outside of the joint what can be advantageous if constructive space is little or not available. The joint mechanism allows a rotation around three axes in the CoR. If axis J_{S3} is defined as TCP (tool center point), a workspace with the radius r_{WSS} is created as shown in green in figure 1.
For the integration of the mechanism into a robot, basic dimensions need to be defined while the functional parameters

need to be set. By rotating the second axis J_{S2}, the third axis leaves the alignment with the first axis and achieves a maximal bending angle β_{WS} that is defined as:

$$\beta_{WS} = 2 \cdot \alpha_S \tag{1}$$

The distance between the slit of the first axis and the CoR marked as H_{CoR} is dependant of α_S and has influence on the curvature of the workspace:

$$H_{CoR}(\alpha_S) = \frac{a_{J1}}{sin(\alpha_S)} \tag{2}$$

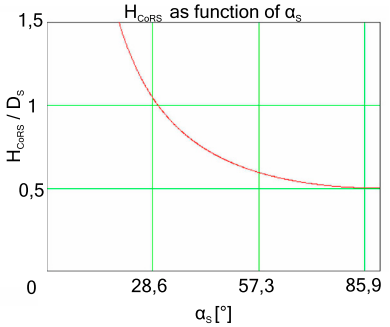

Fig. 2. Relation of the height of the CoR to the axis angle α_S

If the horizontal shift a_{J1} is noted theoretically as half of the mechanisms diameter D_S, the equations together show limitations in the application of the kinematic. If one assumes a given diameter for an application, the maximum bending angle and the height of the CoR are dependent. For applications where balancing is in focus, meaning that the center of mass of the upper structure superimposes with the CoR, the maximum bending angle β_{WS} is defined. The dependency of H_{CoR} of the angle α_S is shown in figure 2 For generalisation the H_{CoR} is normed by D_S. A second important parameter for the integration in a robot is the overall height of the joint mechanism H_S. From the sketch in figure 1, it can be seen that the height H_S is the sum of d_{J1} and h_{J3} with the limitation that the height of the first axis is neglected.

If the goal is to keep the height H_S as small as possible, the axis J_{S3} can be integrated in upper the part of the sphere in a way that $h_{J3} = 0$. With that, the height can be written dependent of the angle α_S:

$$H_S(\alpha_S) = d_{J1}(\alpha_S) = H_{CoR}(\alpha_S) - \sqrt{H_{CoR}(\alpha_S)^2 - a_{J1}^2} \tag{3}$$

This dependency is visualized in figure 3 in which $H_S(\alpha_S)$ is normed by the diameter D_S. The graph shows that the height of the kinematic is nearly linear for values of α_S from $0 \ldots 45°$. For values bigger than 45° the height grows disproportionately high.
From the two displayed dependencies in figure 2 and 3, it can be concluded that the recommended range for the angle α_S is $0 \ldots 45°$ because here the CoR is above the construction and a compact design can be achieved.

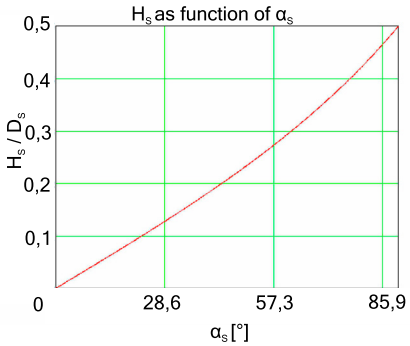

Fig. 3. Relation of the height of the mechanism to the axis angle α_S

3. Comparison to other Joint Mechanisms

The introduced joint mechanism in figure 1 falls between two known kinematics. One is the wedge-shaped joint mechanism shown in figure 4 and used e. g. for painting robots. The difference is that the second axis has no horizontal shift as a_{J1} and has the advantage that a hollow-shaft-design is possible for guiding tubes for paint and air inside a robot arm. The other kinematic is a gimbal joint used e.g. as bearing for marine compass. The difference here is that the angle $\alpha = 90°$.
The parameters height of the mechanism, the height of the CoR and the horizontal displacement of the third axis are

compared. Therefore all parameters are normed to a fix diameter D_i. It is assumed that components like motor and gears fit inside the design. An angle $\alpha_S = 30°$ is chosen for the comparison.

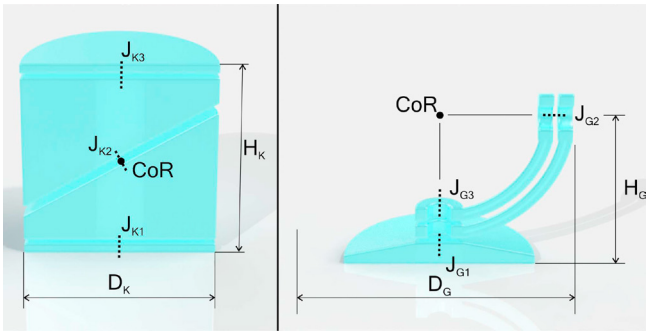

Fig. 4. Left: wedge-shape kinematic. Right: gimbal kinematic

The minimal height of the mechanism for the wedge-shape joint H_K is defined by the angle of the second axis and the diameter D_K. With the given parameters H_K results in $H_K = \frac{\sqrt{3}}{3} \approx 0.577$. The height of the gimbal joint can be defined as the half of the diameter. With equation (3) the height of the spherical joint can be calculated and gives $H_S = 1 - \frac{\sqrt{3}}{3} \approx 0.133$. Since for the wedge-shape mechanism the CoR is located in the junction of the first and second axis, H_{CoR_K} refered to D_K results in $H_{CoR_K} = \frac{\sqrt{3}}{6} \approx 0.289$. The height of the CoR of the gimbal joint equals the height of the mechanism. From equation (2) the height of the CoR of the spherical joint can be calculated and results in $H_{CoR} = 1$.

The horizontal displacement of the end of the kinematic chain is important for an index for bringing cameras that are mounted on top in a position that they can see downwards as it is shown in figure 5. A shift bigger than the half of the diameter means that the center of the top platform is shifted outside of the mechanism and mounted cameras have free view downwards. The horizontal displacement can be calculated for the spherical joint with equation (4) and results in a displacement of $\Delta x_S = 0.643$ referred to the diameter D_S.

$$\Delta x_S = sin(\beta_{WS}) \cdot H_{CoR} \tag{4}$$

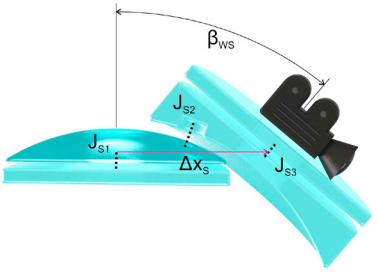

Fig. 5. Visualization of the horizontal shift Δx_i on the example of the spherical joint

For the wedge-shape kinematic, the horizontal shift is $\Delta x_K = 0.186$. The gimbal kinematic allows a shift of $\Delta x_G = 0.321$. All results are shown in table 1. For the compared parameters, the table 1 shows that the spherical joint has the lowest profile ratio, the highest CoR and enables the biggest vertical shift for sensors.

Table 1. Comparison of the mechanism height H_i, the height of the CoR H_{CoR_i} and the horizontal shift Δx_i of the three kinematics referred to the diameter of the design

Parameters	Wedge-shape Kinematic	Gimbal Kinematic	Spherical Joint
H_i	$\frac{\sqrt{3}}{3} \approx 0,577$	0.5	$1 - \frac{\sqrt{3}}{2} \approx 0,133$
H_{CoR_i}	$\frac{\sqrt{3}}{6} \approx 0,289$	0.5	1
Δx_i	≈ 0.186	≈ 0.321	≈ 0.643

4. Kinematic Calculation

For a coordinated motion and control, a mapping between the Cartesian base coordinate system and joint angles is needed. The position and orientation of the TCP (Tool Center Point) can be calculated from the joint angles with Denavit-Hartenberg parameters as already stated in [2]. To calculate the joint velocities $\dot{\vec{\theta}}$ for a desired Cartesian velocity $\vec{v}_e$, the inverse of the Jacobian is needed as it can be seen in equation (5).

$$\dot{\vec{\theta}} = J(\vec{\theta})^{-1} \cdot \vec{v}_e \tag{5}$$

Since the Jacobian matrix is a mapping between Cartesian velocities $\vec{v}_e$ and joint velocities $\dot{\vec{\theta}}$ and dependent on the actual joint angles $\vec{\theta}$, the position can calculated iteratively regarding a time frame Δt as follows.

$$\vec{\theta}(t_{x+1}) = \vec{\theta}(t_x) + J(\vec{\theta}(t_x))^{-1} \cdot \vec{v}_e \cdot \Delta t \tag{6}$$

The inverse of the Jacobian can not be calculated directly because dimension of the matrix is 6×3 and with that not square since the kinematics has three joints and there are six coordinates for the position and orientation of the TCP. Nevertheless, the term $J_O(\vec{\theta}(t_x))^{-1}$ can be calculated using the right inverse as special case of the pseudoinverse matrix calculation. This is a computationally intensive method due to the used singular value decomposition. The proposed method, is to reduce the dimensions of J to 3×3 so that it is square and can be inverted. That is the case when TCP and CoR are congruent. Under this condition, no linear velocities occur and the submatrix of J only regarding rotational velocities can be used in equation (6). To achieve the congruence of the TCP and the CoR, Denavit-Hartenberg parameters $\vec{a}_J$ and $\vec{d}_J$ as introduced in [2] can be formulated with respect to the main kinematic dimension from the previous section and shown in figure 1. Both parameters are given in equation (7).

$$\vec{a}_J = \begin{bmatrix} a_{J1} \\ sin\left(\frac{\pi}{2} - \alpha_S - asin\left(\frac{h_{J3}}{\sqrt{a_{J1}^2 + h_{J3}^2}}\right)\right) \cdot \sqrt{a_{J1}^2 + h_{J3}^2} \\ 0 \end{bmatrix}$$

$$\vec{d}_J = \begin{bmatrix} d_{J1} \\ cos\left(\frac{\pi}{2} - \alpha_S - asin\left(\frac{h_{J3}}{\sqrt{a_{J1}^2 + h_{J3}^2}}\right)\right) \cdot \sqrt{a_{J1}^2 + h_{J3}^2} \\ H_C oR(\alpha_S) - d_{J1} - h_{J3} \end{bmatrix} \tag{7}$$

The method to reduce the Jacobian matrix to a square matrix requires that desired Cartesian velocities and positions are given as rotational velocities and positions of the three axis of the CoR providing an intuitive description of the motion. A simple bend of the robot system to the front can be achieved by a sequence of equal rotational velocities around norm vector of the sagittal plane. The resulting kinematic description can be used for a whole body control, that is not in focus here.

5. Workspace Evaluation

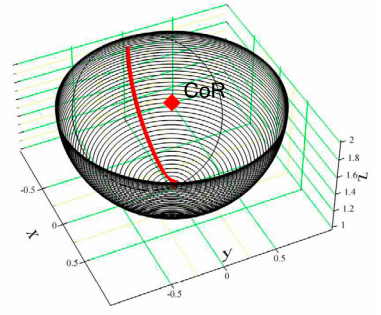

Fig. 6. Workspace of the spherical kinematic.

The workspace of the mechanism is a section of a sphere. Figure 6 exemplary shows it for an angular alignment of $\alpha_S = 45°$. The red line marks the path of the third joint when the mechanism bends. A comparison to other kinematics in [2] shows the differences relatet to the specific application. In general has the mechanism two singularities. One boundary singularity if the links are stretched out or the mechanism is bended. In that case, the end of the kinematics chain reaches the upper end of the path shown in figure 4. In that position, no forces can be applied in the direction of the path but relative velocities orthogonal to the path reach a maximum. The second singularity is an internal singularity in the configuration shown in figure 4 on the lower end of the path when the first and second axis are collinear. The two singularities can limit the capabilities of the mechanism and need to be taken into account in the control. One index to calculate the difference of the capabilities is the manipulability measure $\mu_Y(\vec{\theta})$ proposed in [15]. The index can be used to plan and execute dynamic motions like a fast redirection of the sensors or for gestures.

In contrast to usual applications, it is not desired to avoid the internal singularity since it is the upright and default position, but the curvature of the path near the singularity is limited by the maximal velocity of the first axis. If the direction of the path changes around the singularity, a proportionally fast reconfiguration of the second axis is needed. Typical motions when the TCP swings through the singularity e.g. for nodding or leaning forward and backward if the

robot accelerates or decelerates, are not limited whereby the kinematic is suitable for service robot applications with agile motions.

6. Conclusion and Outlook

Fig. 7. Service robot Care-O-bot 4 Left: Grasping a book. Right: Interacting with a customer.

To evaluate the joint mechanism it was both as torso joint and head joint integrated in the robot Care-O-bot 4 that is shown in figure 7 and applied to real world applications. The small height of the joints enabled a slim and smooth design. The kinematics ensures static stability and a variety of gestures that can be performed that act together with mimics as emotional communication channel. However a whole body control has not been applied jet to enable the full potential. Also a higher control that generates dynamic, natural, humal-like motions would increase the users perception. In the future the mechanism could be used in robot parts e. g. as shoulder or wrist joint of the arms.

References

[1] M. Haegele, World Robotics Report 2017: International Federation of Robotics (IFR), (2017)
[2] T. Fröhlich, U. Reiser: Design and implementation of a spherical joint for mobile manipulators, International Symposium on Robotics, (2016).
[3] E. Ackerman: Robotnik Enters Mobile Manipulator Market With RB-1, Retrieved 2015, March 30 from http://spectrum.ieee.org/automaton/robotics/industrial-robots/robotnik-entersmobile-manipulator-market-with-the-rb1, (2015).
[4] Williow Garage: Robot for Research and Innovation, Retrieved 2015 August 3 from http://www.willowgarage.com/pages/pr2/overview, (2015).
[5] University of Technology Eindhoven: AMIGO, Retrieved 2015 August 3 from http://www.roboticopenplatform.org/wiki/AMIGO, (2015).
[6] Kaweda Industries Inc: Next Generation Industrial Robot - Nextage, Retrieved 2015 August 3 from http://nextage.kawada.jp/en/, (2015).
[7] Honda Motor Co Ltd: ASIMO - The Honda humanoid robot ASIMO, Retrieved 2015 August 3 from http://world.honda.com/ASIMO/, (2014).
[8] PAL Robotics SL: Tiago Mobile Manipulator., Retrieved 2015 March 30 from http://tiago.palrobotics.com/en/, (2015).
[9] Boston Dynamics: Atlas The Agile Anthropomorphic Robot, Retrieved 2015 August 3 from http://www.bostondynamics.com/robotAtlas.html, (2013).
[10] FZI Research Center of Information Technology: HOLLIE - the assistance robot, Retrieved 2015 August 3 from http://www.fzi.de/en/research/projekt-details/hollie/, (2015).
[11] A. Dietrich, M. Kimmel, T. Wimboeck, S. Hirche, A. Albu-Schaeffer: Workspace Analysis for a Kinematically Coupled Torso of a Torque Controlled Humanoid Robot, in Proc. of the IEEE International Conference on Robotics and Automation, (2014) 3439-3445.
[12] J. Kedzierski, R. Muszynski, C. Zoll, A. Oleksy, M. Frontkiewicz: EMYS - Emotive Head of a Social Robot, International Journal of Social Robotics, (2013).
[13] F. Dylan Glas: ERICA: The ERATO Intelligent Conversational Android, Symposium on Human-Robot Interaction, (2015).
[14] U. Reiser, C. Connette, J. Fischer, J. Kubacki, A. Bubeck, F. Weisshardt, T. Jacobs, C. Parlitz, M. Haegele, A. Verl: Care-O-bot 3 - Creating a Product Vision for Service Robot Applications by integrating Design and Technology, IEEE & Robotics Society of Japan IROS, (2009) 1992-1998.
[15] T. Yoshikawa: Manipulability of robotic mechanisms, The International Journal of Robotics Research, (1985).